PROCEEDINGS OF THE YEREVAN STATE UNIVERSITY

Physical and Mathematical Sciences 2019, **53**(1), p. 53–59

P h y s i c s

SELECTION OF COINCIDENCE ELECTRON-PROTON EVENTS IN NUCLEI INTERACTION

D. A. MARTIRYAN[1,2] *

[1] *A. I. Alikhanian National Science Laboratory, Armenia*
[2] *Chair of Nuclear Physics YSU, Armenia*

The main goal of this analysis is to study momentum (or kinetic energy) distribution of the backward going protons using data from CLAS EG2 experiment at Jefferson Lab. In this experiment scattering of a 5.014 *GeV* electron beam off various nucleus targets, ranging from deuterium to lead, have been recorded. The analysis includes selection of events in the reaction $A(e,e',P_{back})X$, where P_{back} is a proton scattered above 90° either in the lab coordinate frame or with respect to the direction of the interacting virtual photon, then performing required corrections and studying the protons momentum distribution as a function of energy transfer. In this paper identification of electron-proton events is presented.

MSC2010: 70G10.

***Keywords*:** backward going protons, CLAS EG2, coincidence electron-proton events.

Introduction. The spectrum of backward scattered protons has been studied since 1970s' with various probes hadron beams at ITEP, FNAL, JINR [1, 2], with photons at YerPhi [3] and with electrons [4, 5]. The common conclusion from all studies was that spectra of protons produced in kinematically forbidden region were very similar. Such protons were called then as "cumulative protons" and it was clear that these protons were coming from the same source in the target nuclei. Later it was determined that these protons were from short-range nucleon correlations in nuclei.

In previous electron and photon scattering measurements, the backward protons had limited momentum range, up to p 1 GeV/c. Using the high statistics of the CLAS EG2 data, one can extend these studies to much higher momentum range ~ 1.5 GeV/c for several nuclei ^{12}C, ^{56}Fe and ^{208}Pb.

The CLAS EG2 experiment has been performed using the CEBAF Large Acceptance Spectrometer, which consists of six sectors, each functioning as an independent magnetic spectrometer. Each sector is instrumented with multiwire drift

* E-mail: davitmartiryan1995@gmail.com

chamber (DC), time-of-flight scintillator counters (SC) covering polar angles $8^\circ < \theta < 143^\circ$, gas-filled threshold Cherenkov counters (CC) and lead-scintillator sandwich-type electromagnetic calorimeters (EC) covering $8^\circ < \theta < 45^\circ$. The calorimeter utilizes a "projective" geometry pointing to the nominal target position that is the area of each successive layer increases linearly with distance. For readout purposes, each scintillator layer consists of 36 strips parallel to one side of the triangle, with orientation of the strips rotated by 120° in successive layers. Thus there are three orientations (labeled U, V and W) each containing 13 layers, which provide stereo information on the location of energy deposition. Each view is further subdivided into an inner (5 layers) and outer (8 layers) stacks to provide longitudinal sampling of the shower for improved electron-hadron separation [6, 7].

The CLAS was triggered on scattered electrons identified by a coincidence between EC and CC signals in a given sector. The way CLAS EG2 target was constructed [8], every solid target was inserted into beam downstream of the cryo-target nonlinear cell. The most of the data on solid targets was taken together with liquid deuterium (LD_2) in the cell.

This analysis is performed using information stored in the output banks of the CLAS simple Event Builder (SEB). The package is part of the CLAS event reconstruction program, preforms several tasks including matching hits and tracks, determination of the event start time and the defining particle IDs and at the end writes out DSTs for physics analysis. In order to select events from LD_2 or a solid target, cuts on the production vertex of particles have to be applied. The CLAS tracking vertex resolution is good enough to isolate tracks produced in the solid targets. The liquid is confined in a Kapton cell that is 2.5 *cm* long and has two 15 μm thick aluminum windows on the way of the beam.

Electron Identification. The electron identification in CLAS relies on reconstruction of a negative track in drift chambers, and hit information from Cherenkov counters and the electromagnetic calorimeters. It is expected to detect more than 2 photo-electrons in Cherenkov PMT from the Cherenkov light that is generated by an election in the working gas of the detector (C_4F_{10}). The electromagnetic calorimeters in other hand will measure energy of the electromagnetic shower from electrons. This energy is proportional to the momentum of the electron. These two signatures and the longitudinal energy distribution in the calorimeter (balance of energies in the inner and outer parts of the calorimeter) are important for final identification of the electron in the event.

The CLAS EC was designed so that electrons and pions had different energy deposition patterns. Electrons produce an electro-magnetic shower where the shower energy is proportional to their momentum, where is pions interact mainly as a minimum ionizing particles (MIP) depositing 2 MeV/cm in the active volume regardless of their momentum.

Electrons selected in the fiducial region (the region of azimuthal angle for a given momentum and polar angle, where the electron detection efficiency is constant) of the CLAS sectors. The fiducial region is defined as the region that is inside the

EC, more than 10 *cm* away from the edges. This is done on all three sides to ensure that the shower produced by a particle is fully contained within the EC. The cut is applied on the coordinate system of the EC (EC–U, EC–V, EC–W). The cut values used are [9]: EC–U $>$ 60 *cm*, EC–V $<$ 360 *cm*, EC–W $<$ 395 *cm*.

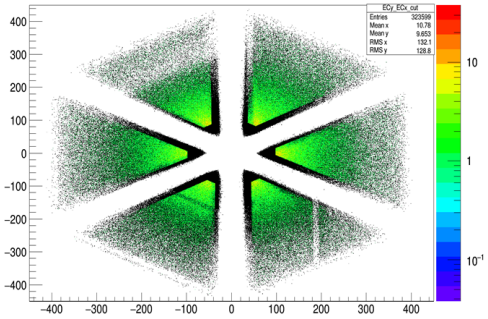

Fig. 1. Fiducial region if the CLAS EC for electron candidates in the global EC_x and EC_y coordinates, where black indicates cuts.

The effect of these cuts on the global EC coordinates (EC_x and EC_y) is shown in Fig. 1. As can be seen, these cuts remove a band of about 10 *cm* off the edges of the calorimeter.

For other cuts that were used for identification of the electron candidate:

- an energy deposit of more than 50 MeV in the inner part of the EC;
- an energy deposit of more than 10 MeV in the outer part of the EC;
- more than 2.5 photo-electrons produced in the CC;
- the momentum normalized energy deposition in the EC,

the ratio EC_{tot}/p was parameterized as a function of momentum, and 3σ cut was applied. Here σ is the Gaussian with of EC_{tot}/p ratio, which also is a function of momentum.

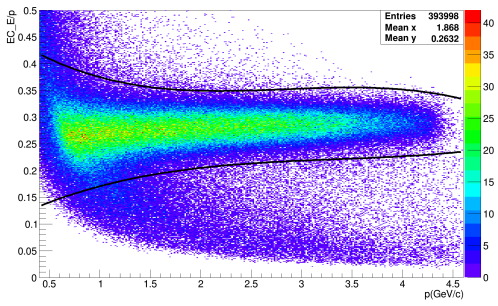

Fig. 2. Momentum normalized total deposit in the EC (E_{tot}/p) vs momentum (p) for the final selected sample of electrons.

The CC is used to better separate electrons and pions. In the radiator used for CC (C_4F_{10}), pions below 2.7 GeV/c will not emit Cherenkov radiation. The average number of photo-electrons ($N_{p.e.}$ or nphe) produced by electron candidates in CC is $\sim 6-7$. The pions produce a peak at $\sim$1.5 p.e., detected by δ emission. The cut of

$N_{p.e.}$>2.5 eliminates most of π^- mesons.

Fig. 2 shows the momentum normalized total deposited energy in the EC (E_{tot}/p) vs momentum for our final selected sample of electrons. Because the shower produced by electrons is proportional to their momentum, as expected this distribution has to be almost constant. The final selection of the electrons is done by cuting around the (EC E_{tot}/p) band with $\pm\,3\sigma$.

Proton Identification. Protons, as well as other long lived charged hadrons, are identified using their time-of-flight (TOF) measured by SC. The TOF measurement is used to assign PIDs in CLAS event builder. This assignment is good to some degree, but for complete analysis it must be checked. In cases that the rate of given process is very small compared to other competing processes or to background, the assigned PIDs may not be good and must be redefined. The common way to check proton identification is to recalculate proton candidates' vertex time at the kinematics of the reaction under analyzes. The vertex time is defined as:

$$\Delta t = t_{SC} - t_{st} - \frac{R_{SC}}{c\beta_c}, \tag{1}$$

where t_{SC} is the time measured by scintillator counter, R_{SC} is the path length of the proton track from the production vertex to the SC; t_{st} is the event start time calculated from the electron time, and the β_c is defined as:

$$\beta_c = \frac{p}{\sqrt{p^2+M^2}}, \tag{2}$$

where $M = 0.938\ GeV$ is the proton mass and p is momentum as measured in the tracking. The vertex time distribution as defined in Eq. (1) for proton candidates as a function of the proton momentum is used to develop cuts for proton identification (see left graph of Fig. 3).

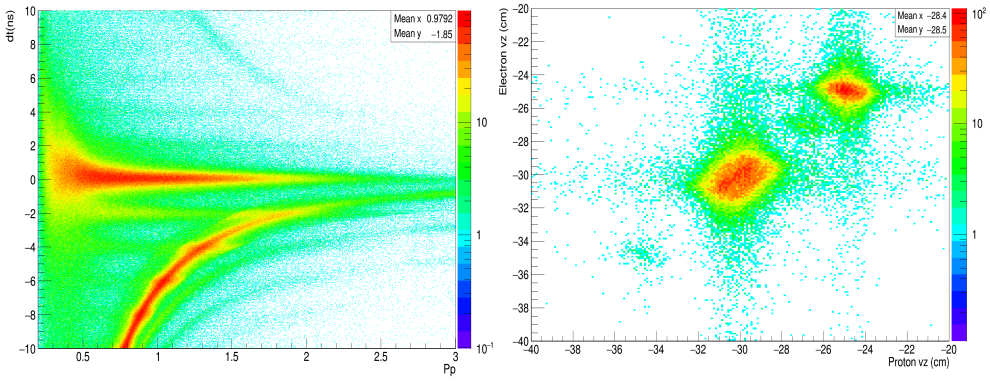

Fig. 3. Proton Vertex time as a function of momentum (without cuts) (left); electron and protons z vertex coincidence from both targets (right).

The mean and the width of the band at "0" is parameterized as a function of momentum. Selection of protons from the band at $\Delta t \approx 0$ will ensure time coincidence of two particles, electron and proton, as they're from the same interaction. One can also see some bands at 2, 4 *ns* and even 6 *ns* on y-axis. These are accidental

protons from the different beam buckets than the electron in the event and should be cut out. The number of such off-time particles will be more at extreme kinematics. So, excluding them will be important, as well as subtracting accidental events that remain under the distribution at 0 (these will be the cases when proton and electrons were produced from different interactions of the same beam bucket). In addition to time coincidence it is required that proton and electron have the same production vertex. In the right graph of Fig. 3 correction between proton and electron z vertex are shown, where correlation between vertexes of two particles is clearly seen.

In order to select proton and electron from the lead target cut was put around the bulb at -25 *cm*, where lead target is located.

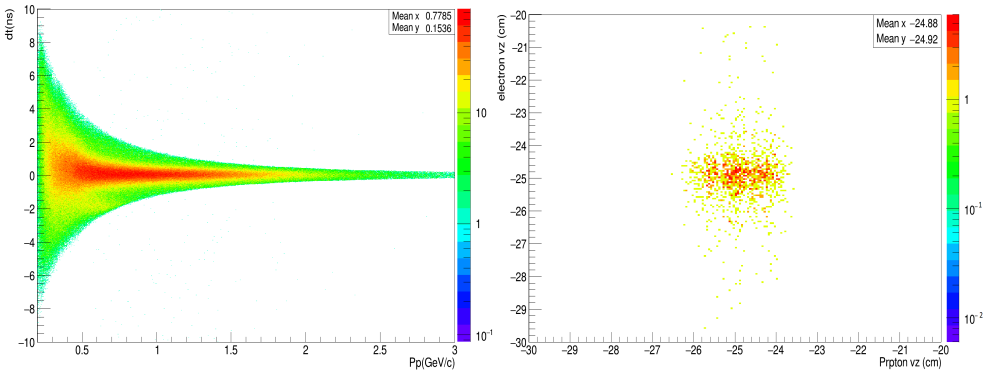

Fig. 4. Proton Vertex time as a function of momentum with cuts (left); electron and protons z vertex coincidence from lead targets (right).

On the left side of Fig. 4 the vertex time distribution around the proton band can be seen and this cut selects electrons and protons coincidence in time within 2 *ns*. On the right graph z vertex distribution of electrons and protons are shown with cut that selects (ep) pair from the same location on the z vertex.

Correction. Besides event selection (for this analysis it is selection of event with an electron and proton from same interaction), there are some corrections that must be applied to some of the measured kinematical quantities. These are momentum corrections for elections, energy loss corrections for protons and correction on z vertex reconstruction. The CLAS tracking system defines vertex as the interaction point of the track with xz plane, where z is in direction of the beam and x is perpendicular to the mid plane of each CLAS sector. This method assumes that beam goes along the z directions, through $x = 0$ and $y = 0$ point at the target. If beam is shifted from $(0,0)$ point, then z vertex of a track will depend on polar and azimuthal angles of the track. This is simple geometrical dependence and can be easily corrected [10]. In addition to that there are tracking issues in very forward going particles that introduces additional dependence of the z vertex and scattering angles in the sector coordinate system.

In left side of Fig. 5 the uncorrected z vertex distribution of the electrons as a function of azimuthal angle ϕ is shown. Besides obvious global ϕ dependence

one can also see dependence within each sector. The correction function has the following form:

$$z^{scorr} = z + z_t + \left(\sum_{i=0}^{i=2} f_i \theta^i + \phi \sum_{i=0}^{i=2} g_i \theta^i \right), \tag{3}$$

where z is the uncorrected z vertex of the electron, $z_t = -24.7$, and parameters f and g are presented in Table. The electron scattering θ and ϕ angles are in degrees.

Sector	f_0	f_1	f_2	g_0	g_1	g_2
1	–25.1797	0.5511E-01	–0.148E-02	–0.10434	0.547E-02	–0.7E-04
2	–24.732	0.118E-02	–0.11E-03	–0.12792	0.1013E-01	–0.21E-03
3	–24.7956	0.291E-02	–0.5E-04	0.10423	–0.58E-02	0.1E-03
4	–24.5825	0.29E-02	–0.31E-03	0.10957	–0.519E-02	0.6E-04
5	–24.9004	0.4239E-01	–0.124E-02	0.1549E-01	0.2E-03	–0.2E-04
6	–25.3849	0.4872E-01	–0.92E-03	0.1581E-01	–0.24E-03	–0.1E-04

After tilted distributions within sectors have been corrected, the next step is to remove trivial ϕ dependence due to beam position on the target not using $x = 0$ and $y = 0$. The correction will be as:

$$z^{corr} = z^{scorr} - \frac{b_1(\cos\phi - b_2)}{\tan\theta}, \tag{4}$$

here $b_1 = 0.361\ cm$ and is the distance of the beam on (xy) from $x = 0$ and $y = 0$ point. The $b_2 = 1.7054$ is the ϕ_b angle of the beam. The right graph of Fig. 5 shows z-ϕ dependence for electrons after all corrections, clearly showing clear separation of liquid target and foils along the beam.

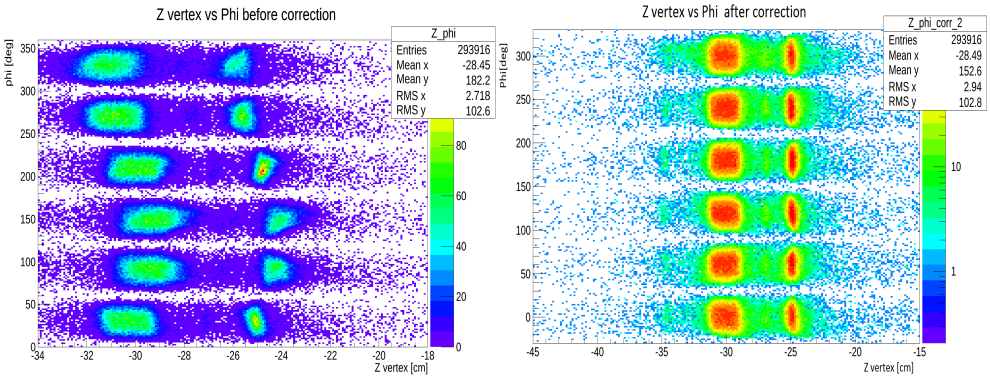

Fig. 5. Uncorrected z vertex of electrons as a function of azimuthal angle ϕ of electron (left); ϕ dependence of the final corrected z vertex of electron (right).

Conclusion. In this work selection of the electron-proton coincidence events in (eA) interactions at 5.014 GeV was established using CLAS data at Jefferson lab. First electrons are identified using Cherenkov and electromagnetic calorimeter detectors from sample of negatively charged tracks reconstructed in CLAS drift

chambers. Then, using electron time as a reference, protons were identified using their TOF from production vertex to the scintillator counters. Fiducial cuts were applied to electron positions in the calorimeter to remove cases when electromagnetic shower was not fully confined in the calorimeter. Besides time coincidence, vertex position cuts were used to make sure electron and proton candidates come from the same production point. In order to improve tracking vertex resolution, angle dependent corrections to z vertex reconstruction were applied.

In the next step of the analysis, these (ep) coincidence events will be used to study kinematics of backward going protons as a function of transferred momentum.

Received 18.12.2018
Reviewed 25.01.2019
Accepted 02.04.2019

REFERENCES

1. **Bayukov Yu.D.** et al. Angular Dependences of Inclusive Nucleon Production in Nuclear Reactions at High-Energies and Separation of Contributions from Quasifree and Deep Inelastic Nuclear Processes. // Sov. J. Nucl. Phys., 1985, v. 42, p. 116–121.
2. **Bayukov Yu.D., Efremenko V.I., Frankel S., Frati W., Gazzaly M., Leksin G.A., Nikiforov N.A., Perdrisat C.F., Chistilin V.I., Zaitsev Yu.M.** Backward Production of Protons in Nuclear Reactions with 400-{GeV} Protons. // Phys. Rev. C, 1979, v. 20, p. 764–772.
3. **Alanakian K.V., Amarian M.Dzh., Demirchyan R.A., Egiian K.Sh., Ogandzhanian M.S., Sharabian Yu.G.** On the Angular Dependence of Photoprotons from Nuclei Irradiated by γ Quanta with Maximum Energy 4.5-{GeV}. // Nucl. Phys. A, 1981, v. 367, p. 429 (in Russian).
4. **Degtyarenko P.V., Efremenko Yu.V., Gavrilov V.B., Leksin G.A., Semenova N.L.** Inelastic Electron-Nucleus Interactions at 5 *GeV* Detected by Argus. // Z. Phys. A, 1990, v. 335, p. 231–238.
5. **Degtyarenko P.V.** et al. Multiple Hadron Production by 14.5 *GeV* Electron and Positron Scattering from Nuclear Targets. // Phys. Rev. C, 1994, v. 50, p. R541–R545
6. **Bayukov Y.D.** et al. TBackward Production of Protons in Nuclear Reactions with 400 *GeV* Protons. // Phys. Rev. C, 1979, v. 20, No. 2, p. 764.
7. **Weinstein L.** Semi-Inclusive Reactions: N, Z, Nucleon Momenta, and Pairing. Ph.D Thesis MIT, 1988.
8. **Amarian M.** et al. The CLAS Forward Electromagnetic Calorimeter. // Nucl. Instrum. Meth. A, 2001, v. 460, p. 239–265.
9. **El Fassi L.** et al. Search for the Onset of Color Transparency vi_0 Electroproduction off Nuclei. Approved CLAS Analysis Note, 2011.
10. **Hakobyan H.** et al. A Double-Target System for Precision Measurements of Nuclear Medium Effects. // Nucl. Instrum. Meth. A, 2008, v. 592, p. 218–223.